Mol Cell Biochem (2017) 436:203–213
DOI 10.1007/s11010-017-3169-8

Potential molecular mechanisms mediating the protective effects of tetrahydroxystilbene glucoside on MPP^+-induced PC12 cell apoptosis

Lingling Zhang[1,2] · Linhong Huang[3] · Xiaobing Li[4] · Cuicui Liu[2] · Xin Sun[1] · Leitao Wu[1] · Tao Li[1] · Hao Yang[2] · Jianzong Chen[1]

Received: 4 July 2017 / Accepted: 16 August 2017 / Published online: 29 August 2017

Abstract Our previous work demonstrated that tetrahydroxystilbene glucoside (TSG) was able to effectively attenuate 1-methyl-4-phenylpyridinium (MPP^+)-induced apoptosis in PC12 cells partially via inhibiting reactive oxygen species (ROS) generation. However, the precise molecular mechanisms of TSG responsible for suppressing neuronal apoptosis have not been fully elucidated. To investigate the possible mechanism, we studied the neuroprotective effects of TSG on MPP^+-induced PC12 cells apoptosis and explored the molecular mechanisms that mediated the effects of TSG. Our results showed that treatment with TSG prior to MPP^+ exposure effectively attenuated the cell viability decrease in PC12 cells, reversed the cell apoptosis, and further restored the mitochondria membrane potential (MMP). In addition, TSG remarkably enhanced the anti-oxidant enzyme activities of superoxide dismutase (SOD), catalase (CAT), and glutathione peroxidase (GSH-Px), and efficiently reduced the malondialdehyde (MDA) content in the PC12 cells. Meanwhile, TSG markedly upregulated the Bcl-2/Bax ratio, reversed release of Cytochrome c, and inhibited the activation of caspase-3 induced by MPP^+. Furthermore, TSG significantly inhibited the activation of p38 mitogen-activated protein kinase (p38MAPK) signaling pathway, while extracellular signal-regulated protein kinases (ERK) phosphorylation was not affected. Together, these findings provide the basis for TSG clinical application as a new therapeutic strategy in the treatment of neurodegenerative diseases.

Keywords Parkinson's disease · Tetrahydroxystilbene glucoside · Neuroprotection · PC12 cells · Oxidative stress

Introduction

Parkinson's disease (PD) is one of the most prevalent progressive neurodegenerative diseases leading to impairments in movement including resting tremor, rigidity, bradykinesia, and postural instability [1]. Pathologically, PD is characterized by a severe and progressive loss of dopaminergic neurons in the substantia nigra pars compacta (SpNc) [1]. Currently there is no effectively curative treatment for the disease with high incidence (approximately 2% of the population aged over 65 years). Increasing evidence revealed that understanding the mechanisms involved in the underlying pathogenesis of PD is pivotal for development of effective therapies. Until now, several key mechanisms have been implicated, including oxidative stress, mitochondrial dysfunction, protein misfolding and aggregation, inflammation, excitotoxicity, apoptotic cell death, and loss of trophic support [2]. Amongst these, oxidative stress plays a central role in the pathogenesis of PD [3]. Apart from cell apoptosis and the DNA damage, lipid peroxidation and protein oxidation

✉ Hao Yang
yanghao.71_99@yahoo.com

✉ Jianzong Chen
chenjz2016@126.com

[1] Research Center of Traditional Chinese Medicine, Xijing Hospital, Fourth Military Medical University, Xi'an 710032, China

[2] Translational Medicine Center, Honghui Hospital, Xi'an Jiaotong University, Xi'an 710054, China

[3] Clinical Pharmacy, Honghui Hospital, Xi'an Jiaotong University, Xi'an 710054, China

[4] Department of Interventional Radiology, Tangdu Hospital, Fourth Military Medical University, Xi'an 710038, China

in PD are caused by reactive oxygen species (ROS) as a result of neuronal apoptosis [4]. Based on the evident role of oxidative stress in PD pathogenesis, several clinical trials have been mainly conducted using several anti-oxidants. In particular, plant anti-oxidants have become attractive targets for drug development in treatment of neurodegenerative diseases due to their neuroprotective effects in animal models and low levels of toxicity [5, 6].

To investigate the neuroprotective effects of some drug interventions and further possible mechanisms, development of an ideal pathological model will provide a considerable therapeutic insight into drug therapy and etiology of PD. 1-methyl-4-phenyl-1, 2, 3, 6-tetrahydropypridine (MPTP) has been widely used as a dopaminergic neurotoxin which causes a severe Parkinsonian-like syndrome with the loss of dopaminergic cells in animals and humans [7]. 1-methyl-4-phenylpyridinium (MPP^+), an active metabolite of MPTP, inhibits mitochondrial complex I, consequently eliciting abnormal energy metabolism and increased ROS production, finally resulting in a model that closely resembles PD [8]. More importantly, choosing an appropriate cell type is of great importance for this aspect study. PC12 cells, a cell line derived from rat adrenal pheochromocytoma cells, are usually used as a model for dopaminergic neurons because they possess intracellular substrates for the synthesis, metabolism, and transportation of dopamine (DA) [9]. In recent reports, accumulating evidences have suggested that MPP^+ induces cytotoxicity in PC12 cells, which provides a suitable model system in studying neuronal cell death caused by oxidative stress as follows: (1) membrane and nuclear damage; (2) MMP loss and decreased anti-oxidant enzyme activities including superoxide dismutase (SOD), catalase (CAT), and glutathione peroxidase (GSH-Px); and (3) increasing the expression of p-MAPKs and decreasing the p-AKT [10–12]. Therefore, MPP^+-induced PC12 cells apoptosis model was employed in our present study.

Polygonum multiflorum Thunb (PM), also called He Shou Wu, is a famous traditional Chinese medicinal herb and has long been used as a tonic and anti-aging agent in the Orient. Multiple medical studies indicated that PM and its extracts can treat age-related diseases and that its mode of action may be attributed to its anti-oxidant activity [13]. TSG (2,3,5,4′-tetrahydroxystilbene-2-O-β-D-glucoside; Fig. 1), one of the main active ingredients of PM [14], has been reported to exert distinct effects on anti-oxidant [15], anti-inflammatory [16], anti-aging [17], neuroprotection [18], and cardioprotection [19]. Another report also revealed that TSG protects human neuroblastoma SH-SY5Y cells against MPP^+-induced cytotoxicity [20]. Additionally, our previous studies showed that TSG can attenuate the MPP^+-induced apoptosis of PC12 cells by inhibiting ROS generation, which is intimately associated

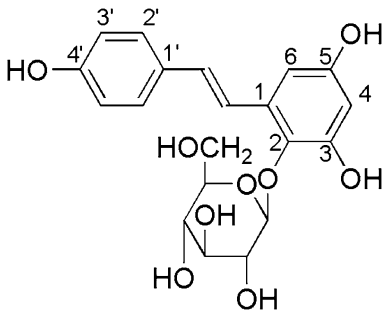

Fig. 1 Schematic diagram of molecular structure of TSG (2, 3, 5, 4′-tetrahydroxystilbene-2-O-β-D-glucoside)

with its modulating activation of Jun N-terminal kinase (JNK) and the PI3K/Akt pathway [12, 15]. Furthermore, the preliminary studies by our group have demonstrated the neuroprotective effects of TSG in the MPTP-induced mouse model of PD [21, 22]. Nonetheless, the molecular mechanisms underlying TSG activity is still elusive.

In the current study, we sought to examine the effects of TSG in the clinically relevant MPP^+-induced in vitro model of PD. We investigated the anti-oxidative stress ability of TSG against MPP^+-induced apoptosis in PC12 cells and the potential molecular mechanisms that might mediate the effects of MPP^+. Of unusual significance, the present study may provide the basis for a new insight into the future clinical application of TSG in the treating PD.

Materials and methods

Reagents and antibodies

Tetrahydroxystilbene glucoside (molecular weight 406, purity >99%) was purchased from the National Institute for the Control of Pharmaceutical and Biological Products (Xi'an, China). Mouse 2.5S nerve growth factor (NGF) was purchased from Promega (Madison, WI, USA). MPP^+, 3-(4, 5-dimethylthiazol-2-yl)-2,5-diphenyl-tetrazolium bromide (MTT), Hoechst 33258, fluorescein isothiocyanate (FITC)-labeled annexin V, propidium iodide (PI), rhodamine 123, and the p38 inhibitor SB203580 were purchased from Sigma-Aldrich Inc. (St. Louis, MO, USA). 0.25% trypsin–EDTA and dimethyl sulfoxide (DMSO) were purchased from Amresco (Solon, OH, USA). The 2,7′-dichlorofluorescin diacetate (DCF-DA), SOD, CAT, MDA, and GSH-Px assay kits were acquired from Beyotime (Nanjing, China). Dulbecco's modified Eagle's medium (DMEM), fetal calf serum (FCS), and horse serum were purchased from Gibco (BRL, USA). Mouse monoclonal antibodies against Bcl-2, Bax, and Cytochrome c were purchased from Santa Cruz Biotechnology (Santa Cruz, CA, USA). Rabbit polyclonal antibodies against p38, p-p38 (Thr180/Tyr182), ERK, p-ERK, cleaved

caspase-3, β-actin, and horseradish peroxidase-conjugated secondary antibodies were purchased from Cell Signaling Technology (Beverly, MA, USA). DAPI (4′, 6-diamidino-2-phenylindole) was obtained from the Nanjing Jiancheng Bioengineering Institute (Nanjing, China). The enhanced chemiluminescence (ECL) reagent and bicinchoninic acid (BCA) protein assay kit were from Pierce (Rockford, IL, USA). All other chemicals used in the present study were of the highest analytical grade and purchased from commercial suppliers.

Cell culture and treatments

PC12 cells were cultured in poly-L-lysine-coated 24 plates in DMEM medium, supplemented with 10% (v/v) heat-inactivated horse serum, 5% (v/v) heat-inactivated FCS, 100 IU/mL of penicillin, and 100 g/mL of streptomycin, in 5% CO_2 with a humidified atmosphere at 37 °C. Culture medium was refreshed every 3 days. When cell confluency reached 60–70%, cells were subcultured for next experiments. Firstly, PC12 cell differentiation was conducted by administration of 50 ng/mL NGF into cultures for 9 days. In parallel, the cells were pretreated with or without of TSG at 5 and 10 μM for 24 h prior to exposure of MPP^+ at a final concentration of 500 μM, and subsequently maintained for another 24 h. To further substantiate the role of the p38 MAPK on the effects of TSG, the cells were pretreated with 2 μM SB203580 (a specific p38 inhibitor) for 0.5 h prior to TSG treatment. For these experiments, control cultures were cultured in DMEM. All experiments were repeated three times for each treatment condition in each experiment.

Cell viability assay

PC12 cells were seeded into 96-well plates at 1×10^4 cells per well and treated with TSG and/or MPP^+. After drug treatment, 20 μL MTT solution (5 mg/mL in PBS) was added into cells and incubated for 4 h. Medium was removed and then 150 μL DMSO was added into the cells. After shaking for 10 min, the optical density (OD) was measured at the absorbance 570 nm using a microplate reader (Bio-Rad, USA). OD value expresses cells viability. Values for each treatment group are expressed as a percentage of the control.

Flow cytometry analysis

To validate TSG protection against MPP^+-induced apoptotic and necrotic cells, PC12 cells treated with TSG were further quantified by dual staining with AV and PI. Briefly, cells were firstly detached from culture plates, harvested, filtered, washed twice with PBS (pH 7.5), and then cell density was adjusted to 1×10^6 cells/mL for detection. After sedimentation and washing in cold PBS (pH 7.5), cells were resuspended in binding buffer (10 mM HEPES–NaOH, pH 7.4, 140 mM NaCl, 2.5 mM $CaCl_2$). Thereafter, 20 μg/mL AV and 50 μg/mL PI were added, and cells were incubated for 15 min at room temperature in the dark. After three wishes with PBS, the cells were analyzed by flow cytometry (Beckman-Coulter, USA) using emission filters 525 and 575 nm for AV and PI, respectively, as described by Yang et al. with minor modifications [23].

Hoechst staining assay

Nuclear morphology changes in apoptotic cells were further investigated by Hoechst 33258 nuclear stain labeling and further examined using fluorescence microscopy. Briefly, after different treatments, PC12 cells grown onto coverslips coated with poly-L-lysine were fixed with 4% (w/v) paraformaldehyde for 30 min, washed three times with PBS (pH 7.5), and then incubated with Hoechst 33258 (3 μg/mL in PBS) for 30 min at room temperature in the dark. After three rinsings with PBS (pH 7.5), nuclear morphology was observed using a fluorescence microscope (Olympus IX71, Japan), and four visual fields were randomly chosen for cell count. Of note, four slides were used for each group. The number of apoptotic cells was expressed as a percentage of the total number of cells.

Measurement of SOD, CAT, GSH-Px activities and MDA level

For measurement of SOD, CAT, GSH-Px activities, and MDA level, PC12 cells were seeded in 6-well plates at a density of 5×10^5 cells/well. After various treatments above-mentioned, the cells were fully washed, collected, and lysed at 4 °C for 30 min. Thereafter, the lysed cells were centrifuged at $10{,}000 \times g$ for 10 min, and the total protein concentration of supernatant was determined using the BCA protein assay kit. Concomitantly, SOD, CAT, GSH-Px activities, and MDA level in the supernatant were further assayed using several different kits, respectively. The measurement was carried out according to manufacturer's instructions (all assay kits were purchased from Beyotime Institute of Biotechnology, Jiangsu, China) [24]. The relative activities of SOD, CAT, GSH-Px were expressed as a ratio to total protein, and the level of MDA was considered as the μmol/mg of total protein as well.

Measurement of mitochondrial membrane potential (MMP)

Mitochondrial activity can be assessed by selective uptake of rhodamine 123, a kind of lipophilic cationic probe,

which requires a negative MMP [25]. After various cell treatments, 10 mg/mL rhodamine 123 was added to the cultures and incubated for 30 min at 37 °C in the dark. Cells were then washed with PBS (pH 7.5) and their mean fluorescence intensity (MFI), representing the MMP, was quantified by flow cytometry (Beckman-Coulter, USA).

Western blotting

Treated cells were briefly washed with PBS (pH 7.5), and extracted in ice-cold RIPA lysis buffer (50 mM Tris–HCl, 150 mM NaCl, 0.02% (w/v) NaN_2, 100 μg/mL phenylmethylsulfonyl fluoride (PMSF), 1 μg/mL aprotinin, and 1% (v/v) Triton X-100). Lysates were clarified by centrifugation, and protein concentration was determined using the BCA assay. Subsequently aliquots of cellular lysate were denatured, separated on a 12% (w/v) polyacrylamide gel and transferred to PVDF membranes. The membranes were incubated in fresh blocking buffer (0.1% Tween 20 in Tris-buffered saline, pH 7.4, containing 5% (w/v) non-fat milk) at room temperature for 1 h and then incubated overnight at 4 °C with primary antibodies (Bcl-2, Bax, cleaved caspase-3, Cytochrome c, p-p38, p38, p-ERK, ERK, and β-actin). After three washes in TBST, membranes were incubated with secondary antibody conjugated to peroxidase at room temperature for 1 h, and labeled proteins were visualized using the ECL detection system. Specific protein expression was estimated by measuring band intensity using densitometer and NIH Image software. For Bcl-2, Bax, Cytochrome c, caspase-3, the optical density of each band was normalized to its respective loading control (β-actin). For p-p38, and p-ERK, was normalized to the total levels of p38, and ERK kinase, respectively.

Statistical analysis

Data are expressed as mean ± standard error of the mean (SEM) from three independent experiments. One-way analysis of variance (ANOVA) followed by the Dunnett's *t* test was used for statistical analysis using SPSS 16.0 software. *p* values <0.05 were considered to be statistically significant.

Results

Effects of TSG on cell viability in NGF-differentiated PC12 cells treated with MPP^+

We recently demonstrated that MPP^+ treatment remarkably decreases the viability of PC12 cells [12, 15]. In agreement with our previous data, in this study, PC12 cell viability decreased by 51.8 ± 1.5% ($p < 0.01$; MPP^+-treated cells vs. untreated control cells) following exposure to 500 μM MPP^+ for 24 h (Fig. 2). To further examine the neuroprotective effects of TSG against MPP^+-induced cytotoxicity, cells were treated with different concentrations of TSG for 24 h prior to incubation with 500 μM MPP^+. Following pretreatment with 5 and 10 μM TSG, the percentage of surviving PC12 cells reached 62.2 ± 2.8% ($p < 0.05$), and 90.8 ± 2.0% ($p < 0.01$), respectively. These results indicate that TSG exhibits dose-dependent neuroprotection of PC12 cells against MPP^+-induced cytotoxicity and that the better rescue dose is at 10 μM. Strikingly, 10 μM TSG treatments alone had no effect on cell viability, indicating that TSG is generally not cytotoxic to PC12 cells.

Effects of TSG on MPP^+-induced apoptosis

To characterize the type and extent of cell death occurrence after MPP^+ treatment, the induction of early apoptotic, late apoptotic, and necrotic cells was quantified using AV and PI double staining and flow cytometry. The results revealed that normal cells were negative for both AV and PI staining (AV^-/PI^-, Q3), early apoptotic cells positive for AV staining and negative for PI staining (AV^+/PI^-, Q4), late apoptotic cells were AV^+/PI^+, Q2 and necrotic cells were AV^-/PI^+, Q1 (Fig. 3a). After 24 h incubation with 500 μM MPP^+, there was a significant increase in the number of apoptotic cells (37.7%) compared with that of the untreated controls (4.1%), while following pre-incubation with 5 and 10 μM TSG, the percentage of apoptotic cells was dramatically reduced to 27.1 and 15.7%, respectively (Fig. 3b).

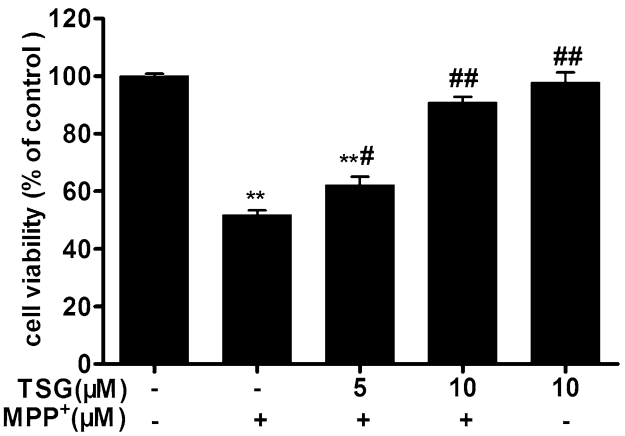

Fig. 2 Effect of TSG on viability of PC12 cells treated by MPP^+ using the MTT assay. The data were represented as mean ± SEM of three independent experiments. $^{**}p < 0.01$ vs. untreated control cells; $^{\#}p < 0.05$ and $^{\#\#}p < 0.01$ vs. MPP^+ alone-treated cells

Effects of TSG on morphology of cell nuclei

In order to characterize the mechanisms that mediate TSG rescue of MPP^+-induced loss of cell viability, we next assessed the effect of MPP^+ treatment on nuclear morphology. Hoechst 33258-stained nuclei in untreated cells were round with regular contours and showed homogeneous and diffuse staining, while MPP^+-induced apoptotic cells exhibited a reduced nuclear size, chromatin condensation, intense fluorescence, and nuclear fragmentation (Fig. 4a). In contrast to untreated cells, cells exposed to 500 μM of MPP^+ for 24 h contained condensed or fragmented nuclei with strong, bright Hoechst 33258 influorescence staining. However, no significant apoptotic nuclei were observed in cells pretreated with different concentrations of TSG (5 or 10 μM). As for PC12 cells treated with TSG alone, no apoptotic cell phenotype was found in visual fields (Fig. 4b).

Effects of TSG on the activity of SOD, CAT, GSH-Px, and MDA level

Effectively scavenging of ROS by several anti-oxidative enzymes, including the three important endogenous enzymes SOD, CAT, and GSH-Px is crucial for cell survial. As shown in Fig. 5a–c, after exposure of PC12 cells to MPP^+, the activities of SOD, CAT, and GSH-Px in cells decreased to 48.80 ± 2.85, 41.00 ± 1.95, and 53.40 ± 2.89%, respectively, as compared to the control group (relative value = 100%). However, pretreatment with TSG significantly increased the activity of SOD (56.60 ± 2.96, 88.60 ± 1.75% for 5 and 10 μM TSG, respectively), CAT (53.60 ± 1.36, 67.20 ± 2.18% for 5 and 10 μM TSG, respectively), and GSH-Px (64.40 ± 2.98, 82.00 ± 2.51% for 5 and 10 μM TSG, respectively). Conversely, the MDA level was significantly increased in MPP^+-treated cells (4.88 ± 0.14 μmol/mg) compared with the control group (2.96 ± 0.20 μmol/mg), whereas TSG could remarkably reduce the MDA production (3.70 ± 0.17 and 2.88 ± 0.15 μmol/mg for 5 and 10 μM TSG, respectively) (Fig. 5d), suggesting that TSG has significant capacity of anti-oxidative stress.

Effects of TSG on MPP^+-induced MMP collapse

Mitochondrial membrane permeabilization constitutes an early event in the apoptotic process, which leads to the dissipation of the inner transmembrane potential and release of soluble intermembrane proteins [26]. To characterize the changes in mitochondrial events induced by TSG pretreatment prior to MPP^+ exposure, the collapse of MMP in PC12 cells was monitored with the rhodamine 123 probe, a specific fluorescent cationic dye that is readily taken up by active mitochondria. Following treatment of PC12 cells with 500 μM

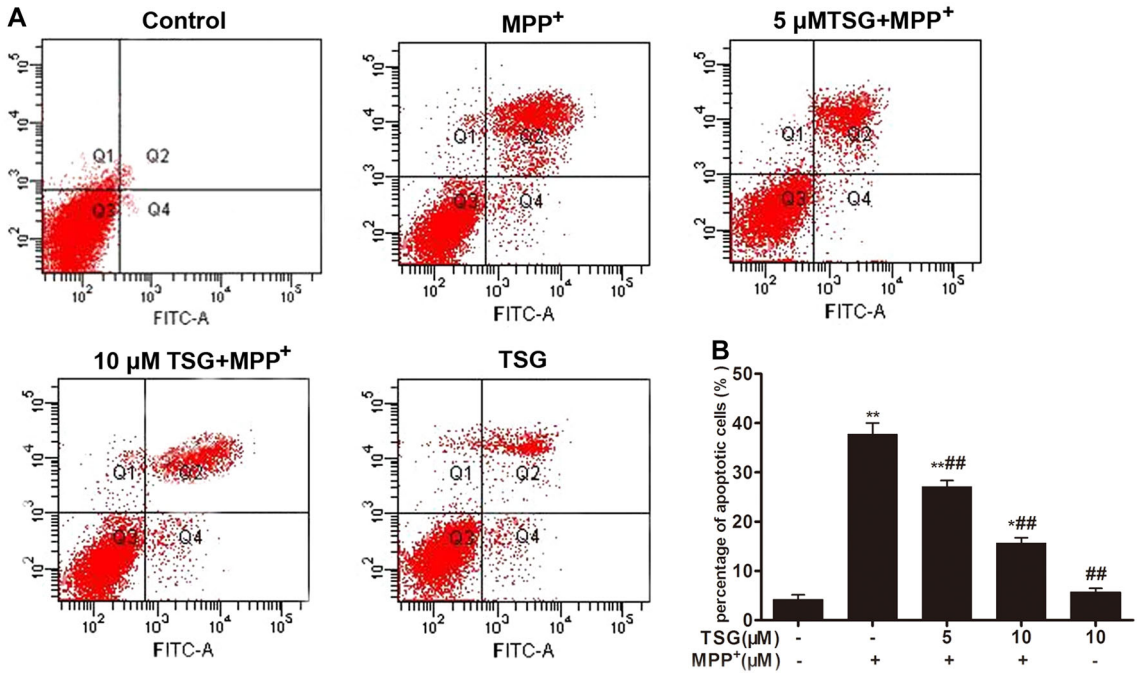

Fig. 3 Flow cytometric analysis of the effect of TSG on MPP^+-induced apoptosis. **a** Representative pictures were obtained from flow cytometry. Representative set of flow cytometric two-parameter *dot-plots*, Annexin V, and PI. The data in each panel represent apoptotic ratio of PC12 at the different treatments **b** quantitative analysis for apoptotic ratio. The data were represented as mean ± SEM of three independent experiments. $^*p < 0.05$ and $^{**}p < 0.01$ vs. untreated corresponding control; $^{\#\#}p < 0.01$ vs. MPP^+ alone-treated cells

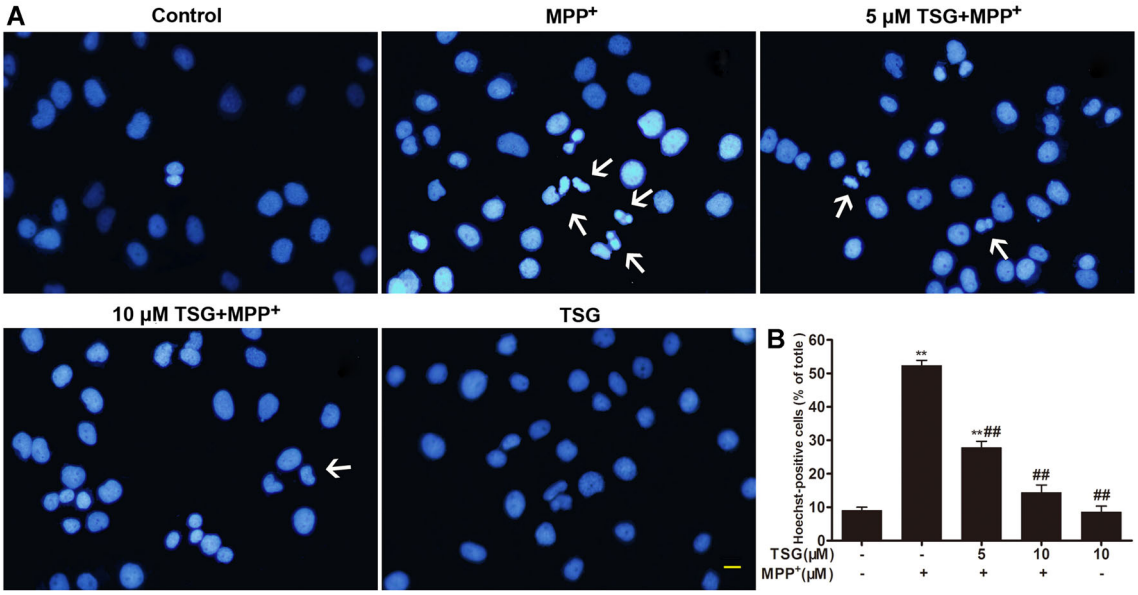

Fig. 4 Inhibitory effects of TSG on MPP^+-induced morphological changes in nuclei **a** representative photographs of PC12 cell nuclear Hoechst 33258 staining following different treatments as indicated. *White arrows* represent morphology of apoptosis cells. **b** Histogram expresses the percentage of cells with condensed nuclei following different treatments. $^{**}p < 0.01$ vs. untreated control cells; $^{\#\#}p < 0.01$ vs. MPP^+ alone-treated cells. *Scale bar* 50 μm

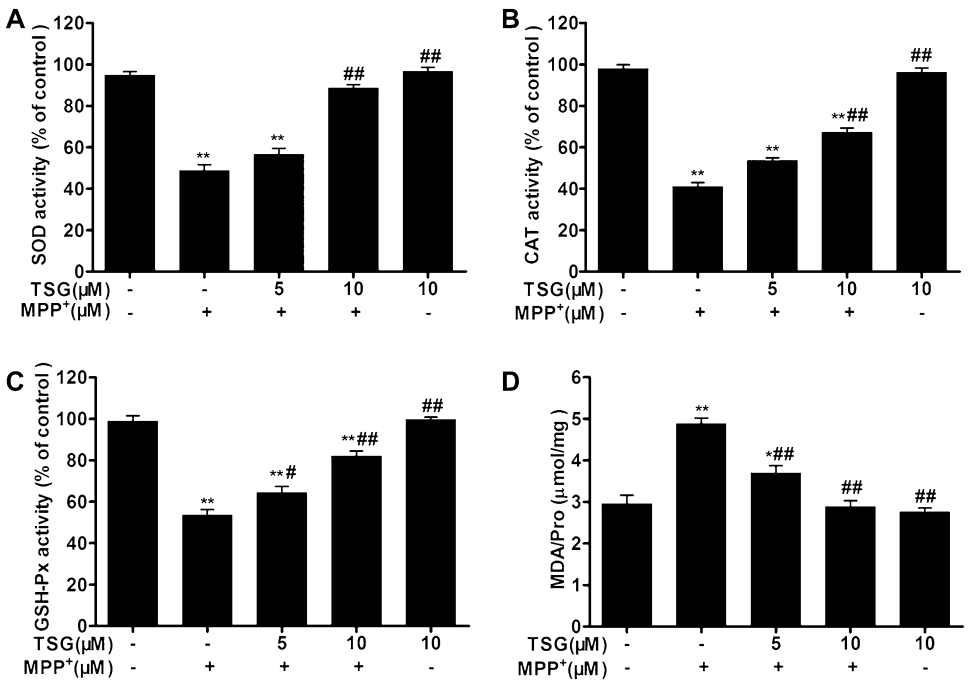

Fig. 5 Effects of TSG on the activity of SOD, CAT, GSH-Px and the MDA level. **a** The SOD activity. **b** The CAT activity. **c** The GSH-Px activity. **d** The MDA level. The data were represented as mean ± SEM of three independent experiments. $^{*}p < 0.05$ and $^{**}p < 0.01$ vs. untreated control cells; $^{\#}p < 0.05$ and $^{\#\#}p < 0.01$ vs. MPP^+ alone-treated cells

MPP^+ for 24 h, rhodamine 123 fluorescence was significantly reduced compared with untreated controls ($p < 0.01$). Pre-treatment with TSG (5 and 10 μM) reversed the reduction in MMP ($^{**,\#\#}p < 0.01$), indicating that TSG treatment protects mitochondria against MPP^+-induced MMP loss (Fig. 6a, b).

The mitochondrial permeability transition pore opening is associated with collapse of the membrane voltage and leads to the release of Cytochrome c into the cytosol [27]. Cytochrome c release has been shown to play a critical role in cell apoptosis. Thus Cytochrome c release was investigated. As shown in Fig. 6c, 500 μM MPP^+ significantly caused Cytochrome c release when compared to the control cells ($p < 0.01$). However, the presence of TSG was able to effectively inhibit its production ($p < 0.05$ and $p < 0.01$ for 5 and 10 μM TSG versus to controls, respectively) (Fig. 6c, d).

Effects of TSG on the expression of apoptosis-related proteins induced by MPP^+

The Bcl-2 family consists of both apoptotic and anti-apoptotic proteins. The balance between these proteins is critical for turning the cellular apoptotic machinery on and off. Any shifts in the balance of pro- and anti-apoptotic factors will cause cell death. It is well known that the Bcl-2/Bax ratio is crucial for initiating apoptosis via the mitochondrial pathway [28]. Therefore, Bcl-2/Bax ratio was determined in the present study. As shown in Fig. 7a and b, the administration of MPP^+ (500 μM) alone obviously decreased Bcl-2/Bax ratio, and the decrease of Bcl-2/Bax ratio induced by MPP^+ was markedly attenuated in cells pretreated with TSG (5 and 10 μM). The qualification analysis further revealed that TSG was able to significantly suppress the decrease of Bcl-2/Bax ratio by MPP^+ treatment ($p < 0.01$ vs. the controls), implying that the MPP^+-induced apoptosis in PC12 is likely mediated by the mitochondrial pathway.

The caspase cascade is the most-studied and best-understood signaling pathway in apoptosis. Caspase-3, a key downstream effector of the cysteine proteinase family, plays a central role in the execution-phase of cell apoptosis [28]. To further substantiate this possibility, expression of caspase-3 levels were further detected. In agreement with changes of Bcl-2/Bax ratio, treatment of 500 μM MPP^+ for 24 h significantly increased expression of cleaved caspase-3 level in PC12 cells compared with untreated controls ($p < 0.01$), while pre-incubation with TSG at 5 and 10 μM remarkably inhibited the increase in cleaved caspase-3 level ($^{**}, ^{\#\#}\ p < 0.01$) (Fig. 7c, d).

Effects of TSG on the MPP^+-induced phosphorylation of p38 and ERK

Our previous research found that TSG might attenuate the MPP^+-induced apoptosis of PC12 cells by inhibiting ROS generation, and modulating the activation of JNK and the PI3K/Akt pathway [12, 15]. In order to further investigate the possible molecular mechanisms underlying TSG's anti-oxidative stress, the expressions of p38 and ERK were investigated by western-blot assay. As shown in Fig. 8a and c, MPP^+ significantly increased the phosphorylation of p38 level, but not on ERK level. Strikingly, pretreatment of TSG significantly inhibited MPP^+-induced phosphorylation of p38. Nevertheless, pretreatment of TSG alone had no significant effect on p38 phosphorylation. Moreover, pretreatment with 2 μM SB203580 (a p38 MAPK inhibitor) effectively inhibited p38 phosphorylation and enhanced the protective effect of TSG. Quantitative analysis further revealed that TSG significantly inhibited MPP^+-induced phosphorylation of p38 level but not on ERK when compared with the corresponding controls ($^*p < 0.05$, $^{**,\ \#\#}p < 0.01$). These results indicated that the p38MAPK signaling pathway is involved in the protective effect of TSG against MPP^+-induced neurotoxicity.

Discussion

Various pharmacological and surgical treatments have been used to treat PD. However, current existing pharmacotherapies have severe adverse effects and do not effectively halt or retard the degeneration of dopaminergic

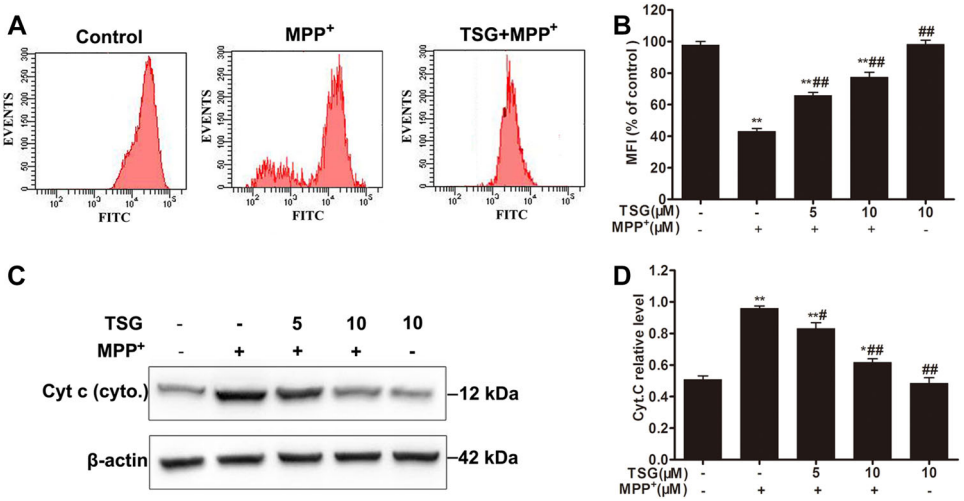

Fig. 6 Effects of TSG on MPP^+-induced MMP collapse and release of Cytochrome c. **a** Representative fluorescence plots showing the shift of the fluorescence intensity peak. **b** Histogram showing the change of MMP by the mean fluorescence intensity (MFI) of rhodamine 123 following different treatments. **c** Western blot analysis of expression of Cytochrome c in PC12 under indicated conditions. The Cytochrome c (cyto). **d** The quantitative analysis of Cytochrome c. The data were represented as mean ± SEM of three dependent experiments. $^*p < 0.05$ and $^{**}p < 0.01$ vs. untreated control sample; $^{\#}p < 0.05$ and $^{\#\#}p < 0.01$ vs. MPP^+ only-treated sample

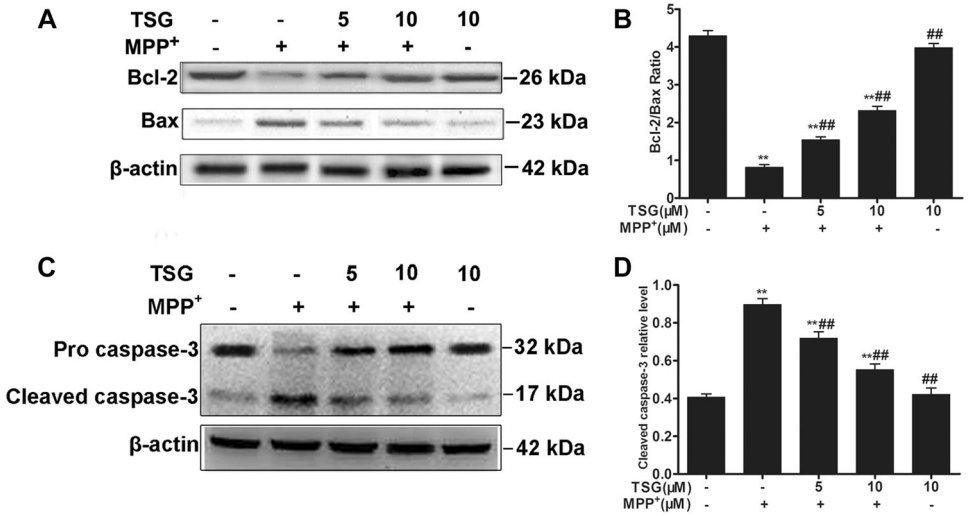

Fig. 7 Effects of TSG on the expression of Bcl-2 and Bax, caspase-3. **a**, **c** The original bands of Bcl-2 and Bax, caspase-3. **b** The quantitative analysis of Bcl-2/Bax ratio. **d** The quantitative analysis of caspase-3. The data were represented as mean ± SEM of three independent experiments. $^{**}p < 0.01$ vs. untreated control sample; $^{\#\#}p < 0.01$ vs. MPP^+ only-treated sample

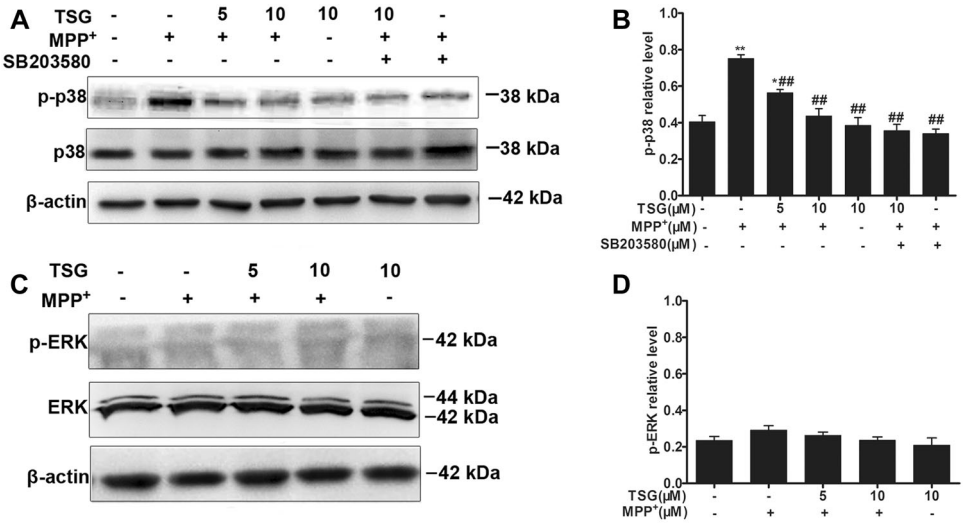

Fig. 8 Effect of TSG on expression of p-38 and p-ERK levels. **a**, **c** Western blot analysis of expression of p-p38 and p-ERK in PC12 cells under indicated various treatments. **b**, **d** Quantification of band intensity, expressed as a fold change relative to untreated controls and normalized to β-actin levels. Total p38 and ERK protein expression levels remained unchanged in each group. The data were represented as mean ± SEM of three independent experiments. $^{*}p < 0.05$ and $^{**}p < 0.01$ vs. corresponding control; $^{\#\#}p < 0.01$ vs. MPP^+ only-treated sample

neurons [29]. In comparison, the traditional medicine as food supplements for health benefits has become attractive in many parts of the world in recent years. Increasing evidence suggests that Chinese herbs and herbal extracts have beneficial effects on neurodegenerative diseases such as PD [30, 31]. *Polygonum multiflorum Thunb* (PM) has long been used as an active constituent of traditional Chinese prescriptions for the treatment of age-related diseases. PM extracts, of which TSG is one of the most important ingredients, exerted protective effect against the MPTP-induced damage of the dopaminergic system of the substantia nigra (SN) in mice, which is a useful animal model of the Parkinsonian phenotype [21, 22]. We previously demonstrated that TSG can exert protective effect against MPP^+-induced damage in PC12 cells in vitro [12, 15]; however, the precise mechanisms underlying this phenomenon required further elucidation.

In our study, we first evaluated the cytotoxic effects of MPP^+ and possibly effects of TSG on PC12 cells by means of MTT assays. Our results showed that the incubation of PC12 cells with TSG prior to exposure of MPP^+ could significantly attenuate cell viability decrease and reverse cell apoptosis in a dose-dependent manner (Figs. 2, 3, 4), suggesting that TSG protects PC12 cells against MPP^+-induced cytotoxicity. Consistently, the subsequent morphological observation of Hoechst 33342 and AV–PI dual staining further supported the results. Interestingly, our results are consistent with previous in vitro reports that

were using different types of cells [12, 15, 20], implicating that TSG has a strong ability of anti-apoptosis.

Our recent studies demonstrated the potential neuroprotective activity of TSG in dopaminergic neurons against the oxidative burden provoked by the administration of MPP^+ or MPTP [15, 22]. An imbalance between the formation of free radicals and reactive oxygen species (ROS) and the body's endogenous anti-oxidant defense mechanisms have also been implicated in the pathogenesis of PD [3, 32]. Thus, anti-oxidant substances can protect cell from pathogenic oxidation. In the brain, the main anti-oxidant enzymes include SOD, CAT, and GSH-Px. Among them, SOD and CAT are the major anti-oxidant enzymes that defend against ROS harmful effects in cells. GSH-Px plays an important role in protecting membranes from damage of lipid peroxidation. Therefore, the levels of SOD and GSH-Px activity are associated with the ability of the organism to eliminate free radicals. MDA is a kind of by-product of lipid peroxidation induced by free radicals and is widely used as a biomarker of oxidative stress [3]. Based on these reports, we detected changes of these related molecules. In our present study, MPP^+ treatment can cause a significant decrease in the activities of SOD, CAT, and GSH-Px in PC12 cells. However, the decrease of these enzyme activities was markedly suppressed by pretreatment with TSG (Fig. 5a–c). Meanwhile, the content of MDA in cells was also significantly reduced by TSG (Fig. 5d). These results suggest that TSG can attenuate MPP^+-induced oxidative damage via abrogation of intracellular lipid peroxidation and elevation of the anti-oxidant enzymes activity.

Another possible mechanism of the TSG protective effects on PC12 cells might be related to the metabolic activity of mitochondria. Mitochondria are not only the main cellular energy producers but are also considered to be the most important source of free radicals, participate in cell signaling and cell life/death decision [33]. Mitochondrial dysfunction caused by MMP loss can lead to inability of mitochondria to furnish sufficient ATP, abnormality of ions and metabolites transport, as well as enhancement of ROS production, resulting in an initiation of a cascade of damaging events involving lipids, proteins, and nucleic acids [33]. Substantial evidence from both genetic and toxin-induced insults in animal cells as well as postmortem human brain tissue indicates that mitochondrial dysfunction plays a central role in pathophysiology of PD [34]. Under oxidative stress induced by ROS such as MPP^+, the mitochondrion will suffer direct damage, leading to loss of MMP, accelerated generation of ROS, release of several pro-apoptotic factors. These harmful molecules rapidly activate caspases as a result of inducing apoptosis. In the present study, dissipation of MMP induced by MPP^+ was elevated by TSG pretreatment (Fig. 6a, b), thus it could be speculated that bioenergetic deficiencies and metabolite imbalances might be suppressed, and that ROS production might be attenuated following TSG pre-incubation. Bcl-2 is a potent cell death suppressor whereas Bax is a death-promoting factor. Studies revealed that once Bax translocates to the mitochondrial membrane, loss of the MMP will increase, leading to release of Cytochrome c [28, 35]. Based on the point, the Bcl-2/Bax ratio was determined to predict cell apoptosis. In addition, it has also been suggested that the activation of caspase-3 is involved in the impairment of dopaminergic neurons in PD [36]. In the present study, we found that TSG not only increase the ratio of Bcl-2/Bax and but also decrease the release of Cytochrome c induced by MPP^+. More importantly, the expression of caspase-3 in cells was also significantly attenuated when compared to the cells treated with MPP^+ alone (Figs. 6c, d, 7). Therefore, we surmised that TSG may provide neuroprotection at least partially via mitochondria dependent apoptotic pathways.

Reactive oxygen species, as second messengers, are known to activate diverse downstream signaling molecules including MAPKs and NF-κB, and mediate apoptosis [37]. The MAPK family comprises JNK, p38, and ERK [38] which participated in a variety of cellular responses. Recent studies have indicated that MAPK signaling is related to the mechanisms of neurodegenerative disorders, such as stroke and Alzheimer's disease [39, 40]. Moreover, several previous studies also show that MPP^+ could rapidly activate JNK and p38, which may be associated with ROS-mediated cell death [41]. Thus, inhibition of p38 MAPK may suppress MPP^+-induced cell death. Our previous study suggest that TSG was protective against MPP^+-induced toxicity in PC12 cells through suppression of ROS production and inhibition of JNK activation [15]. In the present study, pretreatment with TSG could effectively inhibit MPP^+-induced phosphorylation of p38 (Fig. 8a, b), but did not affect the expression of ERK (Fig. 8c, d), suggesting that the p38 pathway also contributes to TSG-mediated neuroprotection.

In accordance with a recent in vivo report, this study demonstrated that TSG inhibited MPP^+-induced oxidative stress in PC12 cells, as indicated by its ability to increase the cell viability. The effectiveness of TSG against MPP^+-induced oxidative stress may be due to restoring anti-oxidant defense system, thereby attenuate ROS production, improve MMP, and prevent the development of apoptosis. Moreover, mechanisms of TSG neuroprotection effects of TSG against MPP^+-induced apoptosis were related to an increase in the Bcl-2/Bax ratio and decreased level of Cytochrome c, caspase-3 as well as the phosphorylation of p-MAPKs. The data presented in this study further support the protective potential of TSG in experimental models of neurodegeneration. TSG should now be tested in animal

models mimicking the progression of PD before being considered as candidate for a clinical trial to prevent PD disease progression in humans.

Acknowledgements This work was supported by grants from the National Natural Science Foundation of China (No. 81371411 and 81173590).

Compliance with ethical standards

Conflict of interest The authors declare that they have no conflict of interest.

References

1. Lees AJ, Hardy J, Revesz T (2009) Parkinson's disease. Lancet 373:2055–2066
2. Yacoubian TA, Standaert DG (2009) Targets for neuroprotection in Parkinson's disease. Biochim Biophys Acta 1792:676–687
3. Zhou C, Huang Y, Przedborski S (2008) Oxidative stress in Parkinson's disease: a mechanism of pathogenic and therapeutic significance. Ann N Y Acad Sci 1147:93–104
4. Halliwell B, Aruoma OI (1991) DNA damage by oxygen-derived species. Its mechanism and measurement in mammalian systems. FEBS Lett 281:9–19
5. Wang S, He H, Chen L, Zhang W, Zhang X, Chen J (2015) Protective effects of salidroside in the MPTP/MPP (+)-induced model of Parkinson's disease through ROS-NO-related mitochondrion pathway. Mol Neurobiol 51:718–728
6. Kuo HC, Lu CC, Shen CH, Tung SY, Hsieh MC, Lee KC, Lee LY, Chen CC, Teng CC, Huang WS, Chen TC, Lee KF (2016) Hericium erinaceus mycelium and its isolated erinacine A protection from MPTP-induced neurotoxicity through the ER stress, triggering an apoptosis cascade. J Transl Med 14:78
7. Lotharius J, O'Malley KL (2000) The parkinsonism-inducing drug 1-methyl-4-phenylpyridinium triggers intracellular dopamine oxidation. A novel mechanism of toxicity. J Biol Chem 275:38581–38588
8. Cassarino DS, Parks JK, Parker WD Jr, Bennett JP Jr (1999) The parkinsonian neurotoxin MPP^+ opens the mitochondrial permeability transition pore and releases cytochrome c in isolated mitochondria via an oxidative mechanism. Biochim Biophys Acta 1453:49–62
9. Rebois RV, Reynolds EE, Toll L, Howard BD (1980) Storage of dopamine and acetylcholine in granules of PC12, a clonal pheochromocytoma cell line. Biochemistry 19:1240–1248
10. Bournival J, Quessy P, Martinoli MG (2009) Protective effects of resveratrol and quercetin against MPP^+-induced oxidative stress act by modulating markers of apoptotic death in dopaminergic neurons. Cell Mol Neurobiol 29:1169–1180
11. Maghsoudi A, Fakharzadeh S, Hafizi M, Abbasi M, Kohram F, Sardab S, Tahzibi A, Kalanaky S, Nazaran MH (2015) Neuroprotective effects of three different sizes nanochelating based nano complexes in MPP (+) induced neurotoxicity. Apoptosis 20:298–309
12. Qin R, Li X, Li G, Tao L, Li Y, Sun J, Kang X, Chen J (2011) Protection by tetrahydroxystilbene glucoside against neurotoxicity induced by MPP^+: the involvement of PI3K/Akt pathway activation. Toxicol Lett 202:1–7
13. Chan YC, Cheng FC, Wang MF (2002) Beneficial effects of different *Polygonum multiflorum* Thunb. extracts on memory and hippocampus morphology. J Nutr Sci Vitaminol (Tokyo) 48:491–497
14. Yao S, Li Y, Kong L (2006) Preparative isolation and purification of chemical constituents from the root of *Polygonum multiflorum* by high-speed counter-current chromatography. J Chromatogr A 1115:64–71
15. Li X, Li Y, Chen J, Sun J, Li X, Sun X, Kang X (2010) Tetrahydroxystilbene glucoside attenuates MPP^+-induced apoptosis in PC12 cells by inhibiting ROS generation and modulating JNK activation. Neurosci Lett 483:1–5
16. Zhang YZ, Shen JF, Xu JY, Xiao JH, Wang JL (2007) Inhibitory effects of 2,3,5,4′-tetrahydroxystilbene-2-O-beta-D-glucoside on experimental inflammation and cyclooxygenase 2 activity. J Asian Nat Prod Res 9:355–363
17. Zhou X, Yang Q, Xie Y, Sun J, Hu J, Qiu P, Cao W, Wang S (2015) Tetrahydroxystilbene glucoside extends mouse life span via upregulating neural klotho and downregulating neural insulin or insulin-like growth factor 1. Neurobiol Aging 36:1462–1470
18. Wang T, Gu J, Wu PF, Wang F, Xiong Z, Yang YJ, Wu WN, Dong LD, Chen JG (2009) Protection by tetrahydroxystilbene glucoside against cerebral ischemia: involvement of JNK, SIRT1, and NF-κB pathways and inhibition of intracellular ROS/RNS generation. Free Radic Biol Med 47:229–240
19. Song F, Zhao J, Hua F, Nian L, Zhou XX, Yang Q, Xie YH, Tang HF, Sun JY, Wang SW (2015) Proliferation of rat cardiac stem cells is induced by 2, 3, 5, 4′-tetrahydroxystilbene-2-O-β-D-glucoside in vitro. Life Sci 132:68–76
20. Sun FL, Zhang L, Zhang RY, Li L (2011) Tetrahydroxystilbene glucoside protects human neuroblastoma SH-SY5Y cells against MPP^+-induced cytotoxicity. Eur J Pharmacol 660:283–290
21. Zhang L, Huang L, Chen L, Hao D, Chen J (2013) Neuroprotection by tetrahydroxystilbene glucoside in the MPTP mouse model of Parkinson's disease. Toxicol Lett 222:155–163
22. He H, Wang S, Tian J, Chen L, Zhang W, Zhao J, Tang H, Zhang X, Chen J (2015) Protective effects of 2,3,5,4′-tetrahydroxystilbene-2-O-β-D-glucoside in the MPTP-induced mouse model of Parkinson's disease: involvement of reactive oxygen species-mediated JNK, P38 and mitochondrial pathways. Eur J Pharmacol 767:175–182
23. Yang YW, Wu CA, Morrow WJ (2004) The apoptotic and necrotic effects of tomatine adjuvant. Vaccine 22:2316–2327
24. Hu XL, Niu YX, Zhang Q, Tian X, Gao LY, Guo LP, Meng WH, Zhao QC (2015) Neuroprotective effects of Kukoamine B against hydrogen peroxide-induced apoptosis and potential mechanisms in SH-SY5Y cells. Environ Toxicol Pharmacol 40:230–240
25. Bass DA, Parce JW, Dechatelet LR, Szejda P, Seeds MC, Thomas M (1983) Flow cytometric studies of oxidative product formation by neutrophils: a graded response to membrane stimulation. J Immunol 130:1910–1917
26. Zamzami N, Kroemer G (2004) Methods to measure membrane potential and permeability transition in the mitochondria during apoptosis. Methods Mol Biol 282:103–115
27. Mignotte B, Vayssiere JL (1998) Mitochondria and apoptosis. Eur J Biochem 252:1–15
28. Hengartner MO (2000) The biochemistry of apoptosis. Nature 407:770–776
29. Toulouse A, Sullivan AM (2008) Progress in Parkinson's disease—where do we stand? Prog Neurobiol 85:376–392
30. Chen LW, Wang YQ, Wei LC, Shi M, Chan YS (2007) Chinese herbs and herbal extracts for neuroprotection of dopaminergic neurons and potential therapeutic treatment of Parkinson's disease. CNS Neurol Disord Drug Targets 6:273–281
31. Heng Y, Zhang QS, Mu Z, Hu JF, Yuan YH, Chen NH (2016) Ginsenoside Rg1 attenuates motor impairment and neuroinflammation in the MPTP-probenecid-induced parkinsonism mouse model by targeting α-synuclein abnormalities in the substantia nigra. Toxicol Lett 243:7–21

32. Kumar H, Lim HW, More SV, Kim BW, Koppula S, Kim IS, Choi DK (2012) The role of free radicals in the aging brain and Parkinson's disease: convergence and parallelism. Int J Mol Sci 13:10478–10504
33. Kroemer G, Galluzzi L, Brenner C (2007) Mitochondrial membrane permeabilization in cell death. Physiol Rev 87:99–163
34. Exner N, Lutz AK, Haass C, Winklhofer KF (2012) Mitochondrial dysfunction in Parkinson's disease: molecular mechanisms and pathophysiological consequences. EMBO J 31:3038–3062
35. Ola MS, Nawaz M, Ahsan H (2011) Role of Bcl-2 family proteins and caspases in the regulation of apoptosis. Mol Cell Biochem 351:41–58
36. Hartmann A, Hunot S, Michel PP, Muriel MP, Vyas S, Faucheux BA, Mouatt-Prigent A, Turmel H, Srinivasan A, Ruberg M, Evan GI, Agid Y, Hirsch EC (2000) Caspase-3: a vulnerability factor and final effector in apoptotic death of dopaminergic neurons in Parkinson's disease. Proc Natl Acad Sci USA 97:2875–2880
37. Eguchi M, Monden K, Miwa N (2003) Role of MAPK phosphorylation in cytoprotection by pro-vitamin C against oxidative stress-induced injuries in cultured cardiomyoblasts and perfused rat heart. J Cell Biochem 90:219–226
38. Chang L, Karin M (2001) Mammalian MAP kinase signaling cascades. Nature 410:37–40
39. Irving EA, Bamford M (2002) Role of mitogen- and stress-activated kinases in ischemic injury. J Cereb Blood Flow Metab 22:631–647
40. Zhu X, Lee HG, Raina AK, Perry G, Smith MA (2002) The role of mitogen-activated protein kinase pathways in Alzheimer's disease. Neurosignals 11:270–281
41. Zhai A, Zhu X, Wang X, Chen R, Wang H (2013) Secalonic acid A protects dopaminergic neurons from 1-methyl-4-phenylpyridinium (MPP^+)-induced cell death via the mitochondrial apoptotic pathway. Eur J Pharmacol 713:58–67